nature medicine

LETTERS

Pharmacological inhibition of EGFR signaling enhances G-CSF–induced hematopoietic stem cell mobilization

Marnie A Ryan[1], Kalpana J Nattamai[1], Ellen Xing[1], David Schleimer[1], Deidre Daria[1,2], Amitava Sengupta[1], Anja Köhler[3], Wei Liu[1], Matthias Gunzer[3], Michael Jansen[1], Nancy Ratner[1], Timothy D Le Cras[4], Amanda Waterstrat[5], Gary Van Zant[6], Jose A Cancelas[1,7], Yi Zheng[1] & Hartmut Geiger[1,2]

Mobilization of hematopoietic stem and progenitor cells (HSPCs) from bone marrow into peripheral blood by the cytokine granulocyte colony–stimulating factor (G-CSF) has become the preferred source of HSPCs for stem cell transplants[1–9]. However, G-CSF fails to mobilize sufficient numbers of stem cells in up to 10% of donors, precluding autologous transplantation in those donors or substantially delaying transplant recovery time[2]. Consequently, new regimens are needed to increase the number of stem cells in peripheral blood upon mobilization. Using a forward genetic approach in mice, we mapped the gene encoding the epidermal growth factor receptor (*Egfr*) to a genetic region modifying G-CSF–mediated HSPC mobilization. Amounts of EGFR in HSPCs inversely correlated with the cells' ability to be mobilized by G-CSF, implying a negative role for EGFR signaling in mobilization. In combination with G-CSF treatment, genetic reduction of EGFR activity in HSPCs (in waved-2 mutant mice) or treatment with the EGFR inhibitor erlotinib increased mobilization. Increased mobilization due to suppression of EGFR activity correlated with reduced activity of cell division control protein-42 (Cdc42), and genetic Cdc42 deficiency *in vivo* also enhanced G-CSF–induced mobilization. Our findings reveal a previously unknown signaling pathway regulating stem cell mobilization and provide a new pharmacological approach for improving HSPC mobilization and thereby transplantation outcomes.

Cytokine-induced mobilization of HSPCs is evolutionarily conserved from mice to humans, such that inbred strains of mice are considered a valuable experimental system for studies that can be translated to humans. Much of the current knowledge about the cellular and molecular events regulating G-CSF–induced mobilization comes from studying this process in mice. Using a forward genetic approach and a congenic mouse model, we previously identified linkage between a locus on mouse chromosome 11 and regulation of HSPC mobilization[10]. In a congenic line named B6.D2 chr11 (line G) derived from genetic crosses between C57BL/6 and DBA/2 mice, a 36-Mbp region of chromosome 11 derived from DBA/2 conferred an approximately threefold increase in mobilization (**Fig. 1a**). To further narrow the interval conferring increased mobilization, we generated new subcongenic mice from line G by further backcrossing to C57BL/6 mice[10] (**Fig. 1b**). Mobilization was determined using a standard G-CSF mobilization protocol[10,11] (**Fig. 1c**). Subcongenic lines 106, 1023 and 1804 showed increased mobilization compared to C57BL/6 mice, whereas line 338 had a phenotype similar to that of C57BL/6 (**Fig. 1c**). These data narrow the interval conferring enhanced mobilization to the 14.7–19.5 Mbp region of chromosome 11 (**Fig. 1b**).

Twelve genes are located within this 5-Mbp interval of chromosome 11 (**Supplementary Table 1**). Gene chip expression analyses of 11 of these transcripts (as represented on the Affymetrix MOE430 microarray) revealed differential expression of the genes *Egfr* and *C1d* between line G and C57BL/6 mice (**Fig. 1d**). Because EGFR is known to have a key role in both cell adhesion and migration, we selected it as a potential quantitative trait gene in the interval. By quantitative real-time RT-PCR, we confirmed that *Egfr* expression was decreased in hematopoietic progenitor cells (HPCs) isolated from the bone marrow of line G and line 1804 compared to HPCs of C57BL/6 mice under steady state conditions and, more markedly, upon G-CSF–induced mobilization (**Fig. 1e**). We also found that *Egfr* expression was lower in HPCs compared to other tissues of C57BL/6 mice (**Supplementary Table 2**). These data demonstrate an inverse correlation between *Egfr* expression with mobilization and imply a negative role for EGFR signaling in mobilization.

To test for a possible inhibitory role of EGFR signaling in mobilization, we treated C57BL/6 mice with a combination of G-CSF and epidermal growth factor (EGF). We found a dose-dependent inhibition of HPC mobilization by EGF (**Fig. 2a**). EGF in the dose range tested did not restrict steady-state mobilization in mice not treated with G-CSF (data not shown). To test whether activation of EGFR signaling with EGF reduced stem cell mobilization, we performed competitive transplants with equal volumes of blood from C57BL/6

[1]Division of Experimental Hematology and Cancer Biology, Cincinnati Children's Hospital Medical Center (CCHMC), Cincinnati, Ohio, USA. [2]Department of Dermatology and Allergic Diseases, University of Ulm, Ulm, Germany. [3]Institute of Molecular and Clinical Immunology, Otto von Guericke University, Magdeburg, Germany. [4]Division of Pulmonary Biology, CCHMC, Cincinnati, Ohio, USA. [5]Department of Biological Sciences, Eastern Kentucky University, Richmond, Kentucky, USA. [6]Department of Internal Medicine, Markey Cancer Center, Division of Hematology/Oncology, University of Kentucky, Lexington, Kentucky, USA. [7]Hoxworth Blood Center, University of Cincinnati College of Medicine, Cincinnati, Ohio, USA. Correspondence should be addressed to H.G. (hartmut.geiger@cchmc.org).

Received 10 March; accepted 24 August; published online 26 September 2010; doi:10.1038/nm.2217

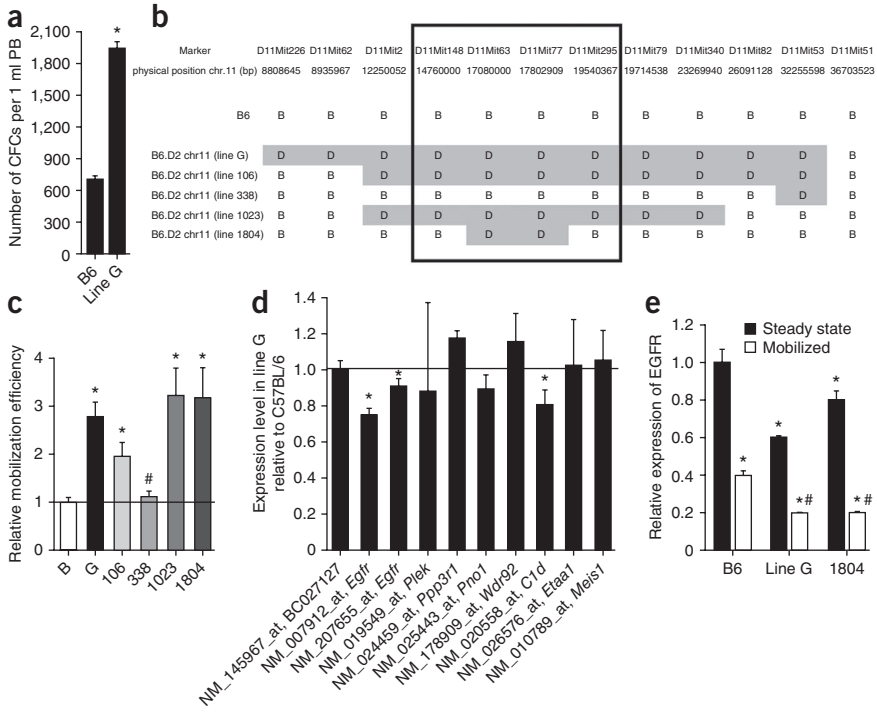

Figure 1 Regulation of G-CSF–mediated mobilization is linked to a 5-Mbp interval on mouse chromosome 11 containing the *Egfr* locus. (**a**) Frequency of CFCs after G-CSF induced mobilization in C57BL/6 (B6, $n = 10$) and line G ($n = 10$) (0–36 Mbp on chromosome 11) mice. $^{*}P < 0.05$ versus C57BL/6. PB, peripheral blood. (**b**) Genetic constitution of C57BL/6.D2 chromosome 11 (line G) and the new subcongenic lines generated from line G (B, C57BL/6 allele, D, DBA/2 allele). The column headings indicate the PCR markers that define the underlying SNPs. The square represents the 5-Mbp interval between 14.7 and 19.5 Mbp. (**c**) G-CSF induced mobilization in subcongenic lines 106 (D2 interval 8.9–36.7 Mbp) ($n = 4$), 338 (D2 interval 26.1–36.7 Mbp) ($n = 7$), 1023 (D2 interval 8.9–26.1 Mbp) ($n = 4$) and 1804 (D2 interval 14.7–19.5 Mbp) ($n = 8$) relative to C57BL/6 and line G. $^{*}P < 0.05$ versus C57BL/6, $^{\#}P < 0.05$ versus line G. (**d**) Relative differences in expression in HPCs ($Lin^{-}c\text{-}Kit^{+}$ cells) from the bone marrow of C57BL/6 and line G mice of the indicated genes in the 5-Mbp interval represented on the MOE430 chip. The level of expression for C57BL/6 set to 1. Data are based on three independent hybridizations per genotype. $^{*}P < 0.05$. *Plek*, plekstrin; *Pno1* partner of NOB1 homolog; *Wdr92*, WD repeat domain 92; *Etaa1*, Ewing tumor-associated antigen-1; *Meis1*, myeloid ectropic viral integration-1. (**e**) *Egfr* expression by quantitative RT-PCR in bone marrow–derived HPCs ($Lin^{-}c\text{-}Kit^{+}$ cells) from C57BL/6, line G and line 1804 mice; for C57BL/6 and line G, $n = 3$ repeats per experimental group (four mice per group); for line 1804, $n = 2$ repeats per experimental group (four mice per group). Steady state refers to expression in HPCs from nonmobilized mice; mobilized refers to expression in HPCs from G-CSF–mobilized mice. $^{*}P < 0.05$ versus C57BL/6 at steady state, $^{\#}P < 0.05$ versus C57BL/6 mobilized. Error bars represent the mean ± s.e.m., except for expression data in line 1804 in **e**, where they represent s.d.

mice treated with G-CSF or with G-CSF and EGF (0.8 μg EGF per g body weight) (**Fig. 2b**). Transplantation of peripheral blood from mice treated with G-CSF and EGF resulted in approximately five-fold less chimerism 3 months after transplant compared to peripheral blood from mice treated with G-CSF alone, corresponding to a decrease in repopulating units (RU)[12] from 1.9 ± 0.7 RU for G-CSF to 0.14 ± 0.07 for G-CSF plus EGF (**Fig. 2c**). As suggested by the reduced EGFR expression in HPCs from line 1804 mice (**Fig. 1e**), these mice were significantly less sensitive to inhibition of mobilization by EGF relative to C57BL/6 mice (**Fig. 2d**). EGFR is activated by several ligands in addition to EGF, including transforming growth factor-α (TGF-α), betacellulin and heparin-binding EGF

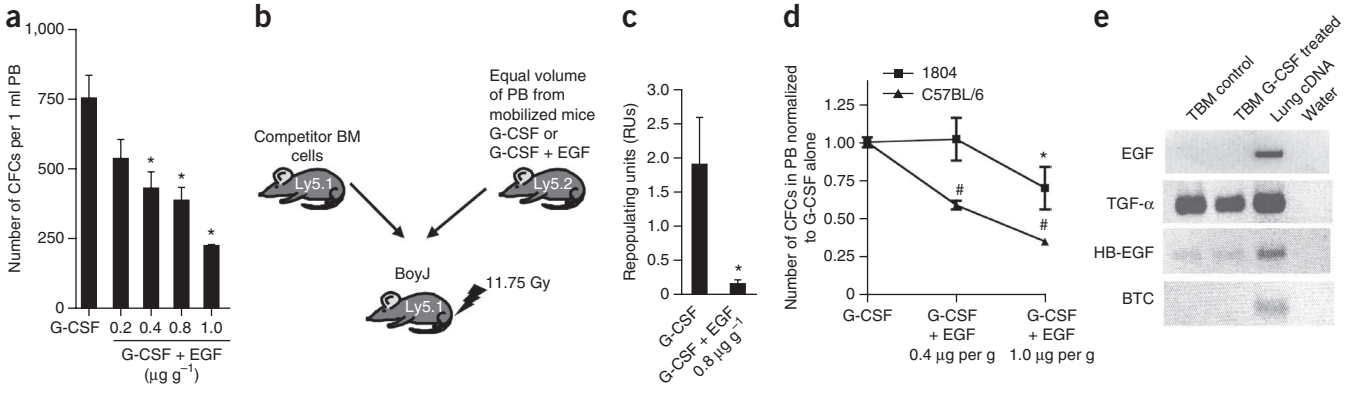

Figure 2 EGF reduces G-CSF–induced mobilization of HSPCs. (**a**) Mobilization efficiency of C57BL/6 mice after a single dose of EGF on day 5 of the standard G-CSF regimen ($n = 6$, at least three mice per group), $^{*}P < 0.05$ versus G-CSF only. (**b**) Schematic of the setup for competitive transplant experiments in **c** to measure repopulating units in peripheral blood using identical volumes of peripheral blood as donor tissue from mice treated with G-CSF ($n = 3$) or G-CSF and EGF ($n = 4$) in competition with identical numbers of C57BL/6 CD45.1^{+} bone marrow cells. BM, bone marrow. (**c**) Repopulating unit values based on donor chimerism measured by flow cytometry in peripheral blood 3 months after transplant. $^{*}P < 0.05$. (**d**) Mobilization of line 1804 compared to C57BL/6 mice after G-CSF and EGF treatment. $^{\#}P < 0.05$ versus G-CSF alone, $^{*}P < 0.05$ C57BL/6 versus line 1804 at the same dose of EGF. (**e**) Expression of known EGFR ligands in total bone marrow. RT-PCR was performed with specific primers for the genes encoding epidermal growth factor (EGF), TGF-α, HB-EGF and betacellulin (BTC) using cDNA isolated from total bone marrow (TBM) and lung (positive control). Error bars represent the mean ± s.e.m.

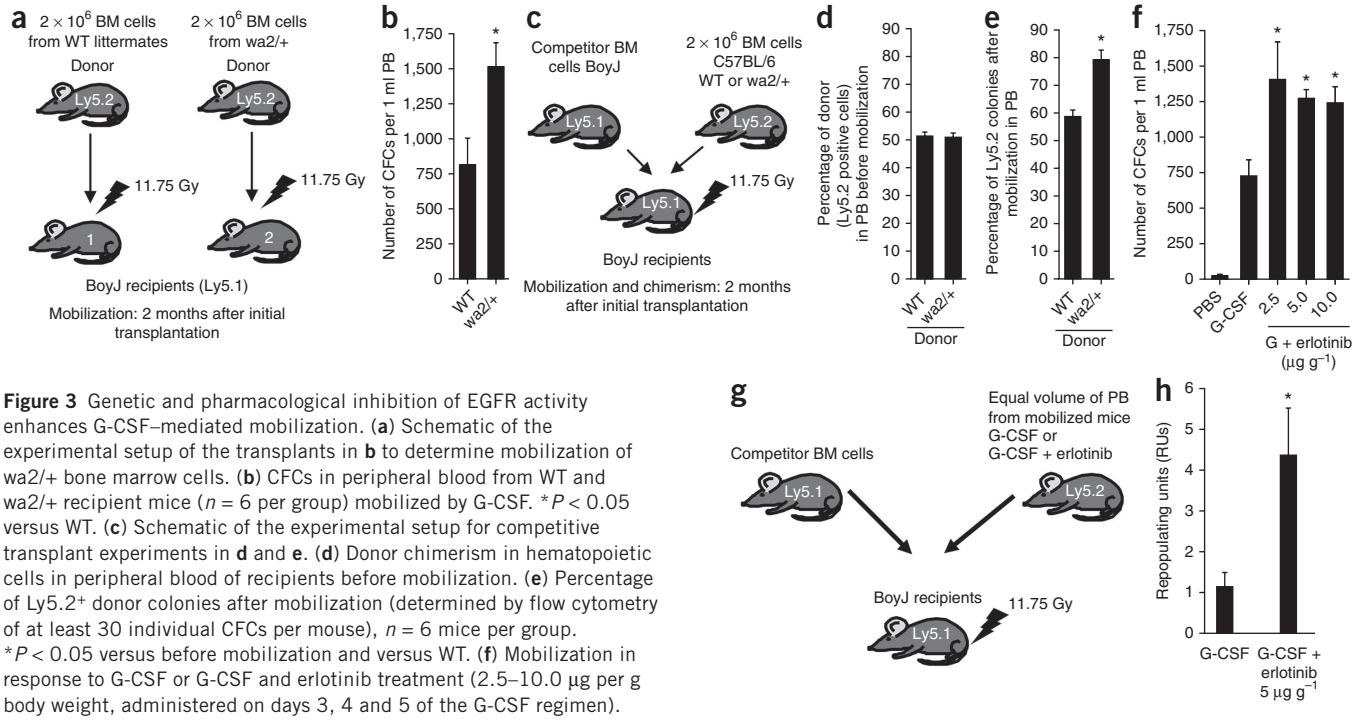

Figure 3 Genetic and pharmacological inhibition of EGFR activity enhances G-CSF–mediated mobilization. (**a**) Schematic of the experimental setup of the transplants in **b** to determine mobilization of wa2/+ bone marrow cells. (**b**) CFCs in peripheral blood from WT and wa2/+ recipient mice ($n = 6$ per group) mobilized by G-CSF. $^*P < 0.05$ versus WT. (**c**) Schematic of the experimental setup for competitive transplant experiments in **d** and **e**. (**d**) Donor chimerism in hematopoietic cells in peripheral blood of recipients before mobilization. (**e**) Percentage of Ly5.2$^+$ donor colonies after mobilization (determined by flow cytometry of at least 30 individual CFCs per mouse), $n = 6$ mice per group. $^*P < 0.05$ versus before mobilization and versus WT. (**f**) Mobilization in response to G-CSF or G-CSF and erlotinib treatment (2.5–10.0 μg per g body weight, administered on days 3, 4 and 5 of the G-CSF regimen). $^*P < 0.05$ versus G-CSF. (**g**) Schematic of the setup for competitive transplant experiments in **h** to measure hematopoietic stem cell frequency in peripheral blood after mobilization by G-CSF or G-CSF plus erlotinib (5 μg per g body weight) in competition with identical numbers of C57BL/6 CD45.1$^+$ bone marrow cells, $n = 3$ repeats per experimental group (three recipient mice per group). (**h**) Repopulating units based on donor chimerism determined by flow cytometry in peripheral blood 3 months after transplant. $^*P < 0.05$ versus G-CSF. Error bars represent the mean ± s.e.m.

(HB-EGF)[12]. Expression of TGF-α and HB-EGF mRNAs, but not of EGF or betacellulin mRNAs, was detected by RT-PCR in bone marrow cells (**Fig. 2e**). Expression array analyses previously revealed expression of EGF in bone marrow stromal cells[13]. Thus, multiple EGFR ligands are found in bone marrow.

The overall goal of these studies was to identify therapeutic targets to increase stem cell mobilization. To test the hypothesis that inhibition of EGFR signaling would enhance mobilization, we used both genetic and pharmacological approaches. As a genetic model we used mice that are heterozygous for the waved-2 mutation in *Egfr* (wa2/+ mice) a strain that has a spontaneous mutation in the tyrosine kinase domain of EGFR, substantially reducing receptor activity[14]. To determine the consequences of reduced EGFR signaling in hematopoietic cells on mobilization, we reconstituted B6.SJL(BoyJ) Ly5.1 recipient mice with either littermate control or wa2/+ bone marrow (**Fig. 3a**). Mice reconstituted with wa2/+ bone marrow showed a significant increase in mobilization compared to controls (**Fig. 3b**). Steady-state levels of colony-forming cells (CFCs) in bone marrow were similar in C57BL/6, line G and wa2/+ mice, indicating that the increase mobilization in line G or wa2/+ HPCs is related to the number of HPCs in BM prior to mobilization (data not shown).

To determine whether the *Egfr* mutation affects mobilization by acting in bone marrow cells or HPCs, as predicted from our previously published experiments analyzing mobilization in congenic line G[10], or alternatively in bone marrow stromal cells, we performed competitive transplants and mobilizations with bone marrow cells from wa2/+ or wild-type (WT) mice (Ly5.2) admixed with competitor bone marrow cells (Ly5.1) (**Fig. 3c**). Donor chimerism was 50% in both cases (**Fig. 3d**), but a significantly higher frequency of Ly5.2 CFCs were mobilized in mice reconstituted with wa2/+ bone marrow (80%) compared to mice reconstituted with WT bone marrow (60%) (**Fig. 3e**), with a 2.6-fold increase in wa2/+ CFCs in peripheral blood upon mobilization relative to control CFCs (calculations according to ref. 12). We also saw a similar skewing toward wa2/+ CFCs in spleen and bone marrow after mobilization (**Supplementary Fig. 1a–c**) as well as in the Lin$^-$c-Kit$^+$ HPC compartment in peripheral blood (**Supplementary Fig. 1d**). Mobilization of neutrophils, which are thought to supply the secondary signals leading to HSPC mobilization upon G-CSF treatment[15], was not altered in wa2/+ competitive mobilization experiments (**Supplementary Fig. 1e,f**) suggesting that EGFR signals through a neutrophil-independent pathway in G-CSF–induced mobilization. Although these data support a primarily HPC-intrinsic role of inhibition of EGFR signaling in enhancing mobilization, these data do not exclude the possibility that additional cell-extrinsic or systemic effects of reduced EGFR signaling influence HSPC mobilization efficiency.

To determine whether pharmacological inhibition of EGFR activity results in enhanced mobilization, C57BL/6 mice were mobilized with G-CSF and treated with erlotinib, a specific inhibitor of EGFR activity[16]. Treatment with erlotinib (2.5–10 μg per g body weight) during the G-CSF regimen increased mobilization of HPCs (**Fig. 3f**). This treatment also increased mobilization of hematopoietic stem cells, as assessed by competitive transplantation of cells mobilized to peripheral blood, with an RU value of 1.1 ± 0.4 for G-CSF compared to RU values of 4.4 ± 1.2 and 7.6 ± 2.5 for erlotinib (5 μg and 10 μg per g body weight, respectively) (**Fig. 3g,h** and **Supplementary Fig. 2**). Erlotinib did not promote mobilization in the absence of G-CSF (**Supplementary Fig. 3**), implying that the action of erlotinib on mobilization depends on additional unidentified factors induced by G-CSF. Notably, whereas inhibition of G-CSF–induced mobilization by EGF or activation of mobilization by erlotinib resulted in an approximately twofold change in mobilization of HPCs (**Figs. 2a** and **3f**),

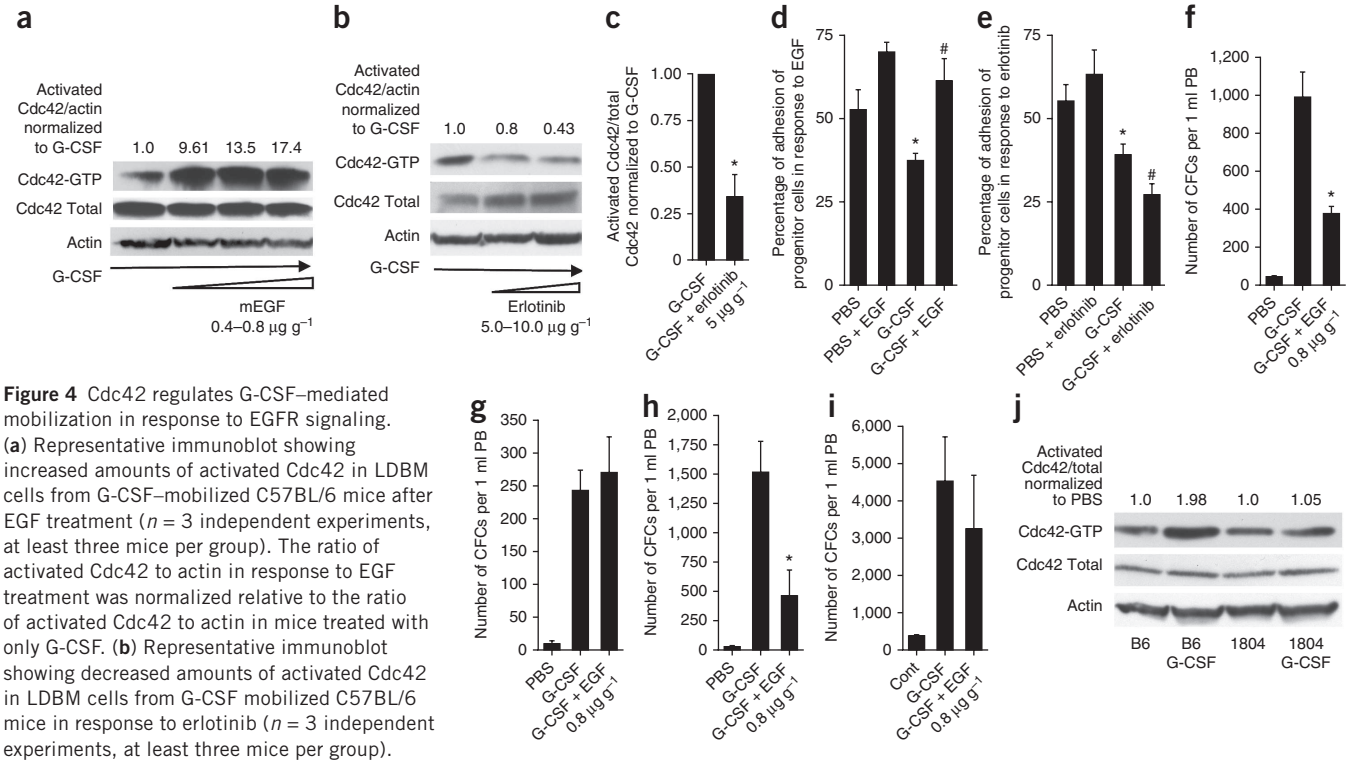

Figure 4 Cdc42 regulates G-CSF–mediated mobilization in response to EGFR signaling. (**a**) Representative immunoblot showing increased amounts of activated Cdc42 in LDBM cells from G-CSF–mobilized C57BL/6 mice after EGF treatment ($n = 3$ independent experiments, at least three mice per group). The ratio of activated Cdc42 to actin in response to EGF treatment was normalized relative to the ratio of activated Cdc42 to actin in mice treated with only G-CSF. (**b**) Representative immunoblot showing decreased amounts of activated Cdc42 in LDBM cells from G-CSF mobilized C57BL/6 mice in response to erlotinib ($n = 3$ independent experiments, at least three mice per group). The ratio of activated Cdc42 to actin in response to erlotinib treatment was normalized relative to the ratio of activated Cdc42 to actin in mice treated with only G-CSF. (**c**) Quantification of the amount of the activated (GTP-bound) form of Cdc42 in LDBM cells upon G-CSF– or G-CSF plus erlotinib (5.0 μg per g body weight)-induced mobilization. Statistical analyses are based on three independent western blots from three independent experiments with three mice in each group. $^{*}P < 0.05$. (**d**) Quantification of progenitor cell adhesion to a layer of FBMD-1 stromal cells after G-CSF or G-CSF and EGF (200 ng ml^{-1}) treatment, $n = 4$ experiments. $^{*}P < 0.05$ versus PBS, $^{\#}P < 0.05$ versus G-CSF. (**e**) Quantification of progenitor cell adhesion to a layer of FBMD-1 stromal cells after G-CSF or G-CSF plus erlotinib (10 μM) treatment (data represent at least three separate experiments). $^{*}P < 0.05$ versus PBS, $^{\#}P < 0.05$ versus G-CSF. (**f**) Frequency of CFCs in peripheral blood in WT mice (littermates) mobilized with G-CSF and treated with EGF (0.8 μg per g body weight) on day 5. $n = 3$ experiments, at least three mice per group, $^{*}P < 0.05$. (**g**) Frequency of CFCs in peripheral blood of wa2/+ mice mobilized with G-CSF and treated with EGF (0.8 μg per g body weight) on day 5. $n = 3$ experiments, at least three mice per group. (**h**) Frequency of CFCs in peripheral blood of WT-reconstituted C57BL/6.SJL(BoyJ) mice in response to G-CSF or G-CSF plus EGF after treatment with polyI:C. $n = 3$ experiments, at least three mice per group, $^{*}P < 0.05$ versus G-CSF. (**i**) Frequency of CFCs in peripheral blood of mice reconstituted with *Cdc42*$^{-/-}$ hematopoietic cells and treated with polyI:C ($n = 12$ mice per group). $P = 0.4715$ G-CSF versus G-CSF plus EGF. (**j**) Representative immunoblots showing the amount of activated Cdc42 in LDBM cells in response to G-CSF in 'poor mobilizer' C57BL/6 mice and the 'better mobilizer' line 1804 (representative of two individual experiments with three mice per group). The ratio of activated Cdc42 to actin was normalized relative to the ratio of activated Cdc42 to actin in PBS (control)-treated C57BL/6 mice. Error bars represent the mean ± s.e.m.

up to a fivefold change in repopulating units occurred in response to these pharmacological treatments (**Figs. 2c** and **3h**), implying a larger effect of EGFR signaling on the mobilization of stem than on progenitor cells. One explanation for this difference might be that changes in EGFR signaling alter the homing or engraftment ability of HSCs or both when transplanted into the recipient animal. Another explanation might be that HSCs are more sensitive to changes in EGFR signaling compared to HPCs.

To identify possible mechanisms by which EGFR signaling alters mobilization, we examined known downstream targets of EGFR signaling, which include the family of small Rho GTPases (Rac1, Rac2 and Cdc42; refs. 17–19). Changes in the activity of these proteins have previously been shown to play a key part in the migration and adhesion of HSPCs[6,20,21]. We performed effector domain pull-down experiments to determine whether activation of EGFR signaling affects the activity of the Rho GTPases (**Fig. 4**). Mobilization by G-CSF resulted in increased activity of Cdc42 in C57BL/6 mice (**Fig. 4j**). Consistent with activation of Cdc42 in fibroblasts in response to EGF[19], activation of EGFR signaling by EGF in G-CSF–treated mice further increased Cdc42 activity in low-density bone marrow (LDBM) cells compared to G-CSF treatment alone (**Fig. 4a**). Conversely, inhibition of EGFR signaling by erlotinib decreased the abundance of active Cdc42 compared to mice treated with G-CSF alone (**Fig. 4b**,**c**). Additionally, phosphorylation of p38, a known downstream target of both Cdc42 and EGFR signaling[22,23], was substantially increased upon activation of EGFR by EGF (**Supplementary Fig. 4**). Neither EGF nor erlotinib altered the cellular composition of LDBM (data not shown), excluding altered cellular composition as a cause for altered Cdc42 activity. We did not detect significant changes in the abundance of the GTP-bound forms of Rac1 or Rac2 (data not shown). Collectively, these data demonstrate that changes in EGFR signaling upon G-CSF–induced mobilization affect the amount of active Cdc42 and additional downstream signaling events.

As release of cells from the stroma is a prerequisite for mobilization[24] and Cdc42 is known to be involved in HSPC adhesion, we tested the ability of bone marrow–derived HPCs from G-CSF-treated C57BL/6 mice to adhere to stroma in response to EGF or erlotinib treatment, as assessed with a cobblestone area–forming cell (CAFC) adhesion assay[11]. EGF treatment enhanced adhesion of HPCs from G-CSF–treated mice to stroma (**Fig. 4d**), whereas treatment with

erlotinib reduced adhesion (**Fig. 4e**). Thus, EGFR signaling may alter HSPC mobilization by altering cell adhesion or chemoattraction. Adhesion and chemoattraction of HSPCs is mediated by integrins and chemokine receptors. We measured the expression of integrins α_4 and α_5, the CXCR4 chemokine receptor[25] and CD26 (ref. 26) on $Lin^-c\text{-}Kit^+$ HPCs isolated from G-CSF–treated mice also treated with or without EGF. The effect of EGF treatment on the expression of these proteins was either not significant or, in the case of CD26, less than 10% compared to G-CSF only, and these effects did not correlate with mobilization efficiency (**Supplementary Fig. 5a–d**). These data suggest that additional receptors may be involved in altering cell adhesion upon activation of EGFR signaling, although we cannot exclude the possibility that changes in integrin activation status (which is crucial for the regulation of adhesion[27–31]), rather than changes in integrin abundance at the cell surface, might be involved in EGF-mediated regulation of mobilization efficiency. We also found that activation of EGFR by EGF correlated with a reduction in the percentage of HPCs in the S phase of mitosis (**Supplementary Fig. 5e**), suggesting that changes in cell cycle parameters may also contribute to inhibition of mobilization by EGF[30,31].

We next studied the role of the EGF-EGFR-Cdc42 axis on mobilization using two complementary genetic approaches. First, G-CSF–induced mobilization in WT mice was significantly reduced by treatment with EGF (**Fig. 4f**), whereas mobilization in naive, untransplanted wa2/+ mice was not affected (**Fig. 4g**), implying that inhibition of mobilization by EGF depends on EGFR activity. In contrast to the experiments in which mice reconstituted with wa2/+ bone marrow showed a higher mobilization efficiency compared to mice reconstituted with bone marrow from littermate controls (**Fig. 3a**,**b**), the number of HPCs mobilized in naive wa2/+ mice after G-CSF treatment was reduced in both peripheral blood and spleen compared to littermate controls, whereas the number of bone marrow CFCs was unchanged (**Fig. 4g** and **Supplementary Fig. 6a**,**b**). One possible explanation for these discrepant results with respect to the role of EGFR signaling in mobilization is that constitutively reduced EGFR signaling in bone marrow stromal cells, in contrast to its role in HSPCs, confers reduced mobilization efficiency. To test this hypothesis, we transplanted B6.SJL(BoyJ) Ly5.1 bone marrow cells into wa2/+ or littermate mice and induced mobilization with G-CSF after hematopoietic reconstitution (2 months after transplantation). The number of mobilized HPCs in reconstituted wa2/+ mice was lower than that in reconstituted WT mice (**Supplementary Fig. 6c**,**d**), indicating that constitutively low EGFR signaling either bodywide or specifically in bone marrow stromal cells of the recipient mice, or in both, impairs mobilization and suggests an effect of constitutively low EGFR signaling on bone marrow stromal cells. The effect of constitutively decreased EGFR activity in bone marrow cells with respect to mobilization is thus distinct from the effect of pharmacological transient inhibition of EGFR signaling induced by erlotinib in both bone marrow stromal cells and HSPCs, which resulted in enhanced mobilization (**Fig. 3f–h**). The distinct outcomes of EGFR signaling pathways in bone marrow stromal cells and HSPCs are further supported by the finding that EGFR expression in C57BL/6 $CD45\text{–}Ter119^-$ bone marrow stromal cells, in contrast to HSPCs, was not altered by G-CSF (**Fig. 1e** and **Supplementary Fig. 7a**); that inhibition of G-CSF–induced mobilization by EGF did not result in an altered percentage of bone marrow stromal cells (**Supplementary Fig. 7b**); and that the expression of CXCL12, integrins α_4 and α_5, vascular cell adhesion molecule-1 (VCAM-1) and CD44 in stromal cells was not different in mice treated with G-CSF plus EGF compared to G-CSF alone (**Supplementary Fig. 7b–f** and data not shown)[1,25,32,33].

To unequivocally determine whether Cdc42 is necessary for altering mobilization upon EGFR signaling, we induced mobilization in mice that were selectively deficient in Cdc42 in bone marrow cells including HSPCs. G-CSF–induced mobilization was significantly enhanced in mice reconstituted with $Cdc42^{-/-}$ bone marrow cells compared to mice reconstituted with WT control bone marrow cells (**Fig. 4h**,**i**, $P = 0.03$), and, similarly to data obtained in wa2/+ mice, mobilization of $Cdc42^{-/-}$ HPCs was not significantly inhibited by EGF, unlike WT control cells (**Fig. 4h**,**i**). Consistent with these data, experiments employing a small molecule inhibitor of Cdc42 activity also suggested that erlotinib increases mobilization by reducing Cdc42 activity (W.L., L. Wang, X. Shang, M.A.R., F. Marchioni *et al.*, unpublished data). These data indicate that EGF-EGFR signaling affects mobilization through modulation of Cdc42 activity.

Last, to investigate the role of Cdc42 in our genetic model of interstrain differences in mobilization, we determined the amount of active Cdc42 in G-CSF–treated C57BL/6 and line 1804 congenic mice. Cdc42 activity in LDBM cells was increased in G-CSF–treated C57BL/6 mice relative to untreated mice, whereas it was not altered in 1804 mice (**Fig. 4j**), suggesting that one mechanism of enhancing G-CSF–induced mobilization is through reduction of the amount of active Cdc42.

Mobilization of HSPCs is a quantitative trait, and the mechanisms responsible for the variability in mobilization observed in patients are unclear[34,35]. Using a forward genetic approach, our data demonstrate a role for EGFR signaling in regulating mobilization, in part by regulating Cdc42 activity. The expression of the human EGFR protein is determined primarily by the abundance of its mRNA, which correlates with allelic polymorphisms[36]. Owing to an absence of definitive data on DNA polymorphisms and their functional relevance for the *EGFR* region in the mouse, both changes in EGFR expression as well as differences in EGFR activity might be responsible for the effects on mobilization in our genetic model system. Our data do not exclude that additional genes in the interval on chromosome 11, such as *C1d*, might further regulate mobilization by as yet unknown mechanisms.

Our data support a model in which relative changes in Cdc42 activity in response to EGF or erlotinib, with respect to the elevated baseline level set by G-CSF, are responsible for alterations in mobilization. Although our data point to effects on mobilization via the EGFR-Cdc42 pathway, the activation status of Cdc42 itself is not an indicator for general mobilization efficiency and has to be interpreted within the cellular and molecular context. This view is also supported by the overall context-dependent role of Cdc42 activity in hematopoiesis, as, in addition to our data, previous studies have shown that both the absence of Cdc42 activity in the knockout mouse model as well as elevated Cdc42 activity in aged mice correlate with elevated numbers of HSPCs in peripheral blood[11,21,37,38]. Our data demonstrate that pharmacological inhibition of EGFR signaling enhances stem cell mobilization, suggesting that therapeutic application of EGFR inhibition might improve G-CSF–induced HSPC mobilization and stem cell therapy outcomes.

METHODS

Methods and any associated references are available in the online version of the paper at http://www.nature.com/naturemedicine/.

Accession codes. Microarray data has been deposited in the Array Express database with accession code E-MEXP-2911.

Note: Supplementary information is available on the Nature Medicine website.

ACKNOWLEDGMENTS

This work was supported by a Cincinnati Children's Hospital Medical Center Translational Research Initiative Award to H.G. and M.A.R., grants from the US National Institutes of Health, HL076604 and DK077762 to H.G., AG024950 and HD060915 to G.V.Z. and an American Heart Association established investigator award to T.D.L.C. (0740069N). H.G. is a New Investigator in Aging, and G.V.Z. is a Senior Scholar in Aging of The Ellison Medical Foundation. A.S. is a recipient of the Lady Tata Memorial Trust Fellowship Award. We would like to thank T. Weaver and M.-D. Filippi for discussions and critical comments on the manuscript. We would like to thank B. Hardie for advice on the erlotinib experiments and the Comprehensive Mouse and Cancer Core as well as the Flow Cytometry Core at CCHMC for help with the experiments and OSI Pharmaceuticals for providing erlotinib.

AUTHOR CONTRIBUTIONS

M.A.R. performed most of the experiments with help from K.J.N., A.S., D.S., D.D., W.L. and J.A.C. M.J. and A.W. performed microarray expression analyses. E.X. performed initial experiments on the inhibition of mobilization of EGF and generated the new congenic strains. J.A.C., N.R., T.D.L.C., G.V.Z., M.G., A.K. and Y.Z. consulted on most of the experiments and provided reagents or data for some experiments. H.G. performed some experiments and planned and supervised all experiments.

COMPETING FINANCIAL INTERESTS

The authors declare competing financial interests: details accompany the full-text HTML version of the paper at http://www.nature.com/naturemedicine/.

Published online at http://www.nature.com/naturemedicine/.
Reprints and permissions information is available online at http://npg.nature.com/reprintsandpermissions/.

1. Katayama, Y. *et al.* Signals from the sympathetic nervous system regulate hematopoietic stem cell egress from bone marrow. *Cell* **124**, 407–421 (2006).
2. Broxmeyer, H.E. *et al.* Rapid mobilization of murine and human hematopoietic stem and progenitor cells with AMD3100, a CXCR4 antagonist. *J. Exp. Med.* **201**, 1307–1318 (2005).
3. Adams, G.B. *et al.* Therapeutic targeting of a stem cell niche. *Nat. Biotechnol.* **25**, 238–243 (2007).
4. Carlo-Stella, C. *et al.* Use of recombinant human growth hormone (rhGH) plus recombinant human granulocyte colony-stimulating factor (rhG-CSF) for the mobilization and collection of $CD34^+$ cells in poor mobilizers. *Blood* **103**, 3287–3295 (2004).
5. Bonig, H., Wundes, A., Chang, K.H., Lucas, S. & Papayannopoulou, T. Increased numbers of circulating hematopoietic stem/progenitor cells are chronically maintained in patients treated with the CD49d blocking antibody natalizumab. *Blood* **111**, 3439–3441 (2008).
6. Cancelas, J.A. *et al.* Rac GTPases differentially integrate signals regulating hematopoietic stem cell localization. *Nat. Med.* **11**, 886–891 (2005).
7. Grigg, A.P. *et al.* Optimizing dose and scheduling of filgrastim (granulocyte colony–stimulating factor) for mobilization and collection of peripheral blood progenitor cells in normal volunteers. *Blood* **86**, 4437–4445 (1995).
8. Flomenberg, N. *et al.* The use of AMD3100 plus G-CSF for autologous hematopoietic progenitor cell mobilization is superior to G-CSF alone. *Blood* **106**, 1867–1874 (2005).
9. Breems, D.A. *et al.* Individual stem cell quality in leukapheresis products is related to the number of mobilized stem cells. *Blood* **87**, 5370–5378 (1996).
10. Geiger, H., Szilvassy, S.J., Ragland, P. & Van Zant, G. Genetic analysis of progenitor cell mobilization by granulocyte colony-stimulating factor: verification and mechanisms for loci on murine chromosomes 2 and 11. *Exp. Hematol.* **32**, 60–67 (2004).
11. Xing, Z. *et al.* Increased hematopoietic stem cell mobilization in aged mice. *Blood* **108**, 2190–2197 (2006).
12. Purton, L.E. & Scadden, D.T. Limiting factors in murine hematopoietic stem cell assays. *Cell Stem Cell* **1**, 263–270 (2007).
13. Waterstrat, A., Liang, Y., Swiderski, C.F., Shelton, B.J. & Van Zant, G. Congenic interval of CD45/Ly-5 congenic mice contains multiple genes that may influence hematopoietic stem cell engraftment. *Blood* **115**, 408–417 (2010).
14. Luetteke, N.C. *et al.* The mouse waved-2 phenotype results from a point mutation in the EGF receptor tyrosine kinase. *Genes Dev.* **8**, 399–413 (1994).
15. Liu, F., Poursine-Laurent, J. & Link, D.C. Expression of the G-CSF receptor on hematopoietic progenitor cells is not required for their mobilization by G-CSF. *Blood* **95**, 3025–3031 (2000).
16. Fabian, M.A. *et al.* A small molecule–kinase interaction map for clinical kinase inhibitors. *Nat. Biotechnol.* **23**, 329–336 (2005).
17. Malliri, A. *et al.* The transcription factor AP-1 is required for EGF-induced activation of rho-like GTPases, cytoskeletal rearrangements, motility and *in vitro* invasion of A431 cells. *J. Cell Biol.* **143**, 1087–1099 (1998).
18. Tu, S., Wu, W.J., Wang, J. & Cerione, R.A. Epidermal growth factor–dependent regulation of Cdc42 is mediated by the Src tyrosine kinase. *J. Biol. Chem.* **278**, 49293–49300 (2003).
19. Hall, A. Rho GTPases and the control of cell behaviour. *Biochem. Soc. Trans.* **33**, 891–895 (2005).
20. Yang, F.C. *et al.* Rac and Cdc42 GTPases control hematopoietic stem cell shape, adhesion, migration and mobilization. *Proc. Natl. Acad. Sci. USA* **98**, 5614–5618 (2001).
21. Yang, L. *et al.* Rho GTPase Cdc42 coordinates hematopoietic stem cell quiescence and niche interaction in the bone marrow. *Proc. Natl. Acad. Sci. USA* **104**, 5091–5096 (2007).
22. Natarajan, A., Wagner, B. & Sibilia, M. The EGF receptor is required for efficient liver regeneration. *Proc. Natl. Acad. Sci. USA* **104**, 17081–17086 (2007).
23. Seo, M. *et al.* Cdc42-dependent mediation of UV-induced p38 activation by G protein βγ subunits. *J. Biol. Chem.* **279**, 17366–17375 (2004).
24. Papayannopoulou, T. & Scadden, D.T. Stem-cell ecology and stem cells in motion. *Blood* **111**, 3923–3930 (2008).
25. Christopher, M.J., Liu, F., Hilton, M.J., Long, F. & Link, D.C. Suppression of CXCL12 production by bone marrow osteoblasts is a common and critical pathway for cytokine-induced mobilization. *Blood* **114**, 1331–1339 (2009).
26. Christopherson, K.W. II, Cooper, S. & Broxmeyer, H.E. Cell surface peptidase CD26/DPPIV mediates G-CSF mobilization of mouse progenitor cells. *Blood* **101**, 4680–4686 (2003).
27. Lévesque, J.P., Leavesley, D.I., Niutta, S., Vadas, M. & Simmons, P.J. Cytokines increase human hemopoietic cell adhesiveness by activation of very late antigen (VLA)-4 and VLA-5 integrins. *J. Exp. Med.* **181**, 1805–1815 (1995).
28. Yamaguchi, M. *et al.* Different adhesive characteristics and VLA-4 expression of $CD34^+$ progenitors in G0/G1 versus S+G2/M phases of the cell cycle. *Blood* **92**, 842–848 (1998).
29. Glimm, H., Oh, I.H. & Eaves, C.J. Human hematopoietic stem cells stimulated to proliferate *in vitro* lose engraftment potential during their S/G(2)/M transit and do not reenter G(0). *Blood* **96**, 4185–4193 (2000).
30. Huygen, S. *et al.* Adhesion of synchronized human hematopoietic progenitor cells to fibronectin and vascular cell adhesion molecule-1 fluctuates reversibly during cell cycle transit in *ex vivo* culture. *Blood* **100**, 2744–2752 (2002).
31. Giet, O. *et al.* Increased binding and defective migration across fibronectin of cycling hematopoietic progenitor cells. *Blood* **99**, 2023–2031 (2002).
32. Lévesque, J.P., Takamatsu, Y., Nilsson, S.K., Haylock, D.N. & Simmons, P.J. Vascular cell adhesion molecule-1 (CD106) is cleaved by neutrophil proteases in the bone marrow following hematopoietic progenitor cell mobilization by granulocyte colony–stimulating factor. *Blood* **98**, 1289–1297 (2001).
33. Semerad, C.L. *et al.* G-CSF potently inhibits osteoblast activity and CXCL12 mRNA expression in the bone marrow. *Blood* **106**, 3020–3027 (2005).
34. Roberts, A.W. *et al.* Genetic influences determining progenitor cell mobilization and leukocytosis induced by granulocyte colony–stimulating factor. *Blood* **89**, 2736–2744 (1997).
35. Hasegawa, M., Baldwin, T.M., Metcalf, D. & Foote, S.J. Progenitor cell mobilization by granulocyte colony–stimulating factor controlled by loci on chromosomes 2 and 11. *Blood* **95**, 1872–1874 (2000).
36. Buerger, H. *et al.* Length and loss of heterozygosity of an intron 1 polymorphic sequence of egfr is related to cytogenetic alterations and epithelial growth factor receptor expression. *Cancer Res.* **60**, 854–857 (2000).
37. Wang, L., Yang, L., Filippi, M.D., Williams, D.A. & Zheng, Y. Genetic deletion of Cdc42GAP reveals a role of Cdc42 in erythropoiesis and hematopoietic stem/progenitor cell survival, adhesion and engraftment. *Blood* **107**, 98–105 (2006).
38. Wang, L., Yang, L., Debidda, M., Witte, D. & Zheng, Y. Cdc42 GTPase-activating protein deficiency promotes genomic instability and premature aging-like phenotypes. *Proc. Natl. Acad. Sci. USA* **104**, 1248–1253 (2007).

ONLINE METHODS

Mice. C57BL/6 mice (6–8-weeks-old) were obtained from the US National Cancer Institute, and congenic and subcongenic mice were obtained from laboratory stocks. Mice were housed in the animal barrier facility at CCHMC. C57BL/6.SJL(BoyJ) mice were obtained from the divisional stock (derived from mice obtained from the Jackson Laboratory) or from the US National Cancer Institute (C57BL/6 Ly5.2Cr). Waved-2 mice (wa2/+) were obtained from Jackson Laboratories and housed in the animal barrier facility at CCHMC. Mx-1-Cre;*Cdc42*$^{flox/flox}$ mice were generated as previously described[39]. The Mx-1-Cre;*Cdc42*$^{flox/flox}$ mice had a mixed 129/C57BL/6 background and were then crossed to C57BL/6 mice for at least three generations in pathogen-free conditions. All mouse studies were approved by the Institutional Animal Care and Use Committee at CCHMC.

Mobilization. Mobilization was induced by treating mice with human G-CSF (Amgen) at 12.5 μg ml^{-1} in PBS containing 0.1% BSA and administered intraperitoneally at 100 μg per kg body weight per day once a day for 5 d, and the mice were analyzed on day 6. Mouse recombinant EGF (0.2–3.6 μg per g body weight) (PeproTech) was dissolved in PBS and administered intraperitoneally on the last day of the G-CSF regimen. Erlotinib (2.5–100 mg per kg body weight) (OSI Pharmaceuticals) was dissolved in methylcellulose and administered by gavage on days 3, 4 and 5 of the G-CSF regimen.

Colony forming cell assays. 150 μl of peripheral blood was added to HBSS and mixed with 4 ml of methylcellulose (Stem Cell Technologies) containing 50 ng ml^{-1} recombinant mouse stem cell factor, 10 ng ml^{-1} recombinant mouse interleukin-3 and 10 ng ml^{-1} recombinant human interleukin-6 (PeproTech) and incubated at 37 °C. Samples were plated in triplicate in six-well plates (Falcon) and, between days 7 and 10 after plating, colonies with more than 50 cells were counted. CFC counts were also determined in spleen (1×10^5) by the same protocol.

Transplantation. For competitive transplants, peripheral blood–derived cells or bone marrow collected from the tibiae and femurs of 6- to 8-week-old mice (donor) and C57BL/6.SJL(BoyJ) (competitor) mice were transplanted into BoyJ recipient mice (2×10^6 cells of each competitor and donor) that had been lethally irradiated with a total dosage of 11.75 Gy (7-Gy and 4.75-Gy doses, 4 h apart). Cells were subsequently transplanted into the retro-orbital sinus in a volume of 200 μl in Iscove's modified Dulbecco's medium (IMDM) containing 2% FCS. Eight weeks after transplantation, the chimerism of the peripheral blood was analyzed by flow cytometry of a panel of markers consisting of CD45.2 and B220 for B cells, CD3ε for T cells and Mac-1 and Gr-1 combined for the myeloid lineage cells.

RU values were calculated according to a previously published method[40]. To generate mice with a hematopoietic system devoid of Cdc42, bone marrow (4×10^6 cells) from Mx1-Cre;*Cdc42*$^{flox/flox}$ mice was injected into the tail vein of lethally irradiated recipient C57BL/6.SJL/BoyJ mice. Eight weeks after transplantation, peripheral blood chimerism was analyzed by flow cytometry. Mice with <95% donor reconstitution were not further studied. Mice were consecutively treated with three doses of sterile polyinosinic-polycytidylic acid (polyI:C; Amersham) every other day at 10 μg per g body weight to induce *Cdc42* deletion. Complete (>95%) deletion of the *cdc42* gene in hematopoietic cells was confirmed by PCR analysis, as previously published[co].

Flow cytometry. Immunostaining and flow cytometry analyses were performed according to standard procedures and analyzed on a FACSCanto flow cytometer (BD Biosciences). Monoclonal antibodies to Ly5.2 (clone 104, BD Biosciences, FITC conjugated) and Ly5.1 (clone A20, BD Biosciences, phycoerythrin (PE) conjugated) were used to distinguish donor from recipient and competitor cells. For lineage analysis in hematopoietic tissues, antibodies against CD3ε (clone 145-2C11, PE-Cy7 conjugated), B220 (clone RA3-6B2, allophycocyanin (APC) conjugated), Mac-1 (clone M1/70, APC-Cy7 conjugated) and Gr-1 (clone RC57BL/6-8C5, APC-Cy7 conjugated, all from BD Biosciences) were used. Cell cycle analysis was performed on cells isolated from mice 45 min after BrdU injection and analyzed according to the manufacturer's protocol (BD Biosciences). Cell surface receptor staining was performed with antibodies against CD49d (clone 9C10, PE conjugated), CD49e (clone 5H10-27 (MFR5), PE conjugated), CD26 (clone H194-112, FITC conjugated) and antibody to CXCR4, (551966, PE conjugated; all from BD Biosciences) and analyzed by flow cytometry.

Cobblestone-area forming cell adhesion assays. FBMD-1 cells were seeded in IMDM supplemented with 15% FCS and 5% horse serum (Gibco) at a density of 1,000 cells per well in a 96-well plate. Bone marrow cells were plated onto the FBMD-1 stromal cell line using 3,000, 1,500, 750 or 375 cells per well (15 wells tested at each cell density) in CAFC medium (IMDM supplemented with 20% horse serum (Gibco) and 10^{-5} M hydrocortisone (Sigma)). To determine progenitor cell adhesion, nonadherent cells were washed off the FBMD-1 stroma after 2 h and fresh CAFC medium was added to each well. The frequency of total and adherent HPCs was determined as the frequency of cobblestone areas 7 d after initiation of the assay.

Quantitative reverse transcription PCR. EGFR mRNA abundance was determined by real-time RT-PCR using Taqman Universal PCR reagents (Applied Biosystems, Assay ID Mm00433023_m1).

RT-PCR. Expression of EGFR ligands in total bone marrow was determined by RT-PCR using specific primers for the genes encoding EGF, TGF-α, HB-EGF and betacellulin in cDNA isolated from total bone marrow. Amplification of mRNA encoding mouse EGFR ligands was performed with the following primer sets: EGF sense 5-GAGAGGTGCAGGACCTG-3′ and antisense 5′-CACCAATTGCTGGTGATTTG-3′; TGF-α sense 5′-TGTGTGATAAAGCTGCCTGC-3′ and antisense 5′-CACCCTTTGAGGTTCGTGT-3′; HB-EGF sense 5′-ATAGCTTTGCGCTGTGACCT-3′ and antisense 5′-CACACTCTTTGGTCCCACCT-3′; betacellulin sense 5′-GGAACCTGAGGACTCATCCA-3′ and antisense 5′-GAGCCATTGGTTTCTGGTGT-3′.

Rho-GTPase effector domain pull-down assays. Relative levels of GTP-bound Rac1, Rac2 and Cdc42 were determined by effector pull-down assays. Briefly, low-density bone marrow cells (1×10^7 cells from the upper layer of a Ficoll gradient (density of 1.083, Sigma)) were lysed in an Mg^{2+} lysis-wash buffer (Upstate Cell Signaling Solutions) containing 10% glycerol, 25 mM sodium fluoride, 1 mM sodium orthovanadate and a protease inhibitor cocktail (Roche Diagnostics). Samples were incubated with PAK-1 binding domain–conjugated agarose beads (Upstate Biotech) and bound (activated) as well as unbound (nonactivated) Rho GTPases were detected by immunoblotting with antibodies specific for Rac1 (clone 23A8, Upstate), Rac2 (catalog number NB100-883, Novus Biologicals) and Cdc42 (catalog number 05-542, Upstate). The abundance of protein in the activated state was normalized to the abundance of β-actin (clone AC-15, Sigma), and the relative amount was quantified by densitometry.

Flow cytometric analysis of bone marrow stromal cells. The frequency of nonhematopoietic cells containing osteoblasts, mesenchymal cells and progenitors was quantified by flow cytometry analysis on CD45$^-$Ter119$^-$ bone marrow cells, using APC-conjugated antibody to CD45 (clone 30-F11) and APC-conjugated antibody to Ter119 (clone Ter-119), from e-Bioscience. For quantification of CXCL12-expressing cells, rabbit antibody to mouse CXCL12 (ab25117, Abcam) was used, followed by incubation with donkey rabbit-specific antibody conjugated to PerCP-Cy5.5 (Santa Cruz, sc-45106). In addition, expression of integrin α_4 (clone 9C10), integrin α_5 (clone 5H10-27 MFR5), CD44 (clone IM7) and VCAM-1 (clone 429 MVCAM.A) was analyzed by determining the mean fluorescence intensity ratio compared to the isotype control fluorescence gated on CD45$^-$Ter119$^-$ bone marrow cells. Antibodies were obtained from BD Biosciences unless otherwise stated.

Mesenchymal progenitor cell assay. For the determination of the frequency of colony-forming units of fibroblasts, bone marrow cells were plated in 1 ml of medium containing IMDM, 30% of mesenchymal-selected FCS (Stem Cell Technologies), 10 ng ml^{-1} recombinant mouse EGF, 10 ng ml^{-1} human platelet-derived growth factor-BB and 40% of Methocult (Stem Cell Technologies) supplemented with 2 mM L-glutamine, 100 U ml^{-1} penicillin and 100 mg ml^{-1} streptomycin (Euroclone). Dishes were cultured for 12 d at 37 °C, 5% CO_2 and

100% humidity. Adherent cell clusters were stained with Diff-Quick (Fisher Scientific) and clusters containing >50 cells were counted.

Whole-genome expression analysis. RNA from sorted $Lin^{-}c\text{-}Kit^{+}$ cells was obtained with the Qiagen RNAase micro kit according to the manufacturer's protocol. RNA was subsequently amplified and labeled by the CCHMC Affymetrix core facility and reverse transcribed using a Nugene kit according to the manufacturer's protocol. Labeled cDNA was then hybridized to an MOE430 array (Affymetrix), and raw expression data were collected. Affymetrix .CEL files of the respective microarrays were imported into the statistical programming language R (http://www.r-project.org/) using the Affy Bioconductor (http://www.bioconductor.org/) package. The data were then preprocessed (background corrected, $\log_2$-transformed, quantile-normalized and summarized) by the rma function of the Affy package. The probe sequences were filtered and regrouped during summarization according to RefSeq annotation with custom chip description files (.CDF) for the MOE430 array provided by the Molecular and Behavioral Neuroscience Institute of the University of Michigan (Microarray Lab) (http://brainarray.mbni.med.umich.edu/Brainarray/Database/CustomCDF/genomic_curated_CDF.asp). Differential expression between C57BL/6 and DBA/2 mice of the 11 transcripts contained in the chromosome 11 interval was tested with a two-tailed *t* test for two samples with unequal variance (Welch's *t* test) without multiple testing correction.

Statistical analyses. A paired Student's *t* test was used to determine the significance of the difference between means of two groups. We used one-way analysis of variance to compare means among three or more independent groups. We applied a Newman-Keuls *post hoc* test with Prism4 whenever we conducted multiple comparisons. Values were considered significant when $P < 0.05$.

Additional methods. Detailed methodology is described in the **Supplementary Methods**.

39. Yang, L., Wang, L. & Zheng, Y. Gene targeting of Cdc42 and Cdc42GAP affirms the critical involvement of Cdc42 in filopodia induction, directed migration, and proliferation in primary mouse embryonic fibroblasts. *Mol. Biol. Cell* **17**, 4675–4685 (2006).
40. Yuan, R., Astle, C.M., Chen, J. & Harrison, D.E. Genetic regulation of hematopoietic stem cell exhaustion during development and growth. *Exp. Hematol.* **33**, 243–250 (2005).

doi:10.1038/nm.2217